Electronic supplementary information

Noble metal-free upgrading of multi-unsaturated biomass derivatives at room temperature: Silyl species enable reactivity

Hu Li, Wenfeng Zhao, Wenshuai Dai, Jingxuan Long, Masaru Watanabe, Sebastian Meier*, Shunmugavel Saravanamurugan*, Song Yang*, Anders Riisager

* Corresponding authors. Email:
semei@kemi.dtu.dk (SM); saravana@ciab.res.in (SS); jhzx.msm@gmail.com (SY)

The PDF file includes:

Supplementary Text

Supplementary Text

Materials

Potassium carbonate (K_2CO_3, 99%), sodium carbonate (Na_2CO_3, >99.8%), lithium carbonate (Li_2CO_3, 99.99%), cesium chloride (CsCl, 99.9%), cesium nitrate ($CsNO_3$, 99.9%), cesium formate (CsOOCH, 98%), trimethoxysilane [$(MeO)_3SiH$, 95%], diphenylsilane (Ph_2SiH_2, 98%), triethylsilane (Et_3SiH, 99%), heptamethyltrisiloxane, polymethylhydrosiloxane, levulinic acid (98%), formic acid (99%), *n*-butylamine (99%), 4-chlorobenzamide (>98%), cyclohexylamine (>99%), aniline (>99%), benzylamine (99%), methyl benzoate (99%), methyl *p*-toluate (99%), methyl *p*-formylbenzoate (98%), methyl 4-acetylbenzoate (98%), 4-nitrobenzaldehyde (98%), 2,5-hexanedione (≥99%), methyl 5-formyl-2-furoate (97%), and 2,5-diformylfuran (98%) were purchased from Beijing InnoChem Science & Technology Co., Ltd. All other organic reagents were in analytically pure and used without further purification, unless otherwise noted.

Catalyst characterization

Magnified images were taken using transmission electron microscopy (TEM, JEM-1200EX). Scanning transmission electron microscope and high-angle annular dark-field (STEM-HAADF) images were obtained using an aberration-corrected FEI Tecnai G2 F30 S-TWIN (S)TEM operating at 300 kV.

Computational method

All geometry optimizations and energy calculations were performed at B3LYP/6-311+g (d, p) level by using the Gaussian 09 package [S1]. Considering the zero point corrections (ZPCs) of all the compounds, harmonic vibrational frequency calculations are performed at the same level to that in geometry optimization process.

Table S1. Hydrogenation of biomass derivatives with different metal catalysts. Some representative examples with good performance on selective hydrogenation of biomass derivatives are listed.

Catalyst	H-donor	Temp. (ºC)	Time (h)	Substrate		Product		Ref.
				Type	Conv.(%)	Type	Yield(%)	
Pt@TECN	1 MPa H_2	100	1	Furfural	98	Furfuryl alcohol	97	S2
Cu/MgAlO	4 MPa H_2	150	3	Furfural	>99	Furfuryl alcohol	99	S3
Pt/C	8 MPa H_2	175	0.5	Furfural	99.3	Furfuryl alcohol	47.9	S4
Pd/C	2 MPa H_2	150	4	Furfural	41.2	Furfuryl alcohol	14.4	S5
Pd/C	8 MPa H_2	160	0.5	Furfural	98.4	Tetrahydrofurfuryl alcohol	62.1	S6
Ru/C	4 MPa H_2	150	-	Levulinic acid	-	γ-Valerolactone	30	S7
Au/ZrO_2-VS	Formic acid	180	3	Levulinic acid	-	γ-Valerolactone	99	S8
Cu-ZrO_2	3.5 MPa H_2	200	5	Methyl levulinate	-	γ-Valerolactone	92	S9
Co-pincer	5 MPa H_2	130	48	Cyclohexyl hexanoate	-	Cyclohexanol	99	S10
Fe-PNP	5 MPa H_2	130	3	*N,N*-dimethyl formamide	-	Methanol	>99	S11
Fe-pincer	6 MPa H_2	90	20	Benzonitrile	>99	*N*-benzyl benzaldimine	98	S12
Fe-complex	3 MPa H_2	100	6	Methyl benzoate	>99	Benzyl alcohol	97	S13

Table S2. Selective hydrogenation of ethyl levulinate (EL) to γ-valerolactone (GVL) and 1,4-pentanediol (1,4-PD) via silyl ethers (Si-1 and Si-2) under various conditions. The reaction conditions are as follows: 1 mmol EL, 1.5 equiv. H^- of $(EtO)_3SiH$, 5 mol% catalyst, 2 mL 2-methyltetrahydrofuran (MTHF)

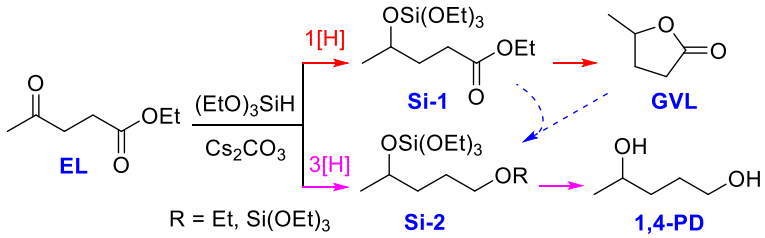

Entry	Catalyst	Temp (ºC)	Time (h)	EL conv. (%)	Product yield (%)				CB[a] (%)
					Si-1	GVL	Si-2	1,4-PD	
1[b]	Cs_2CO_3	25	0.5	98	21	74	<1	0	98
2[c]	Cs_2CO_3	25	0.5	>99	10	87	<1	0	99
3[d]	K_2CO_3	25	0.5	2	<1	1	0	0	>99
4[d]	Na_2CO_3	25	0.5	1	0	<1	0	0	>99
5[d]	Li_2CO_3	25	0.5	0	0	0	0	0	100
6[d]	CsCl	25	1.0	0	0	0	0	0	100
7[d]	$CsNO_3$	25	1.0	0	0	0	0	0	100
8[d]	CsOOCH	25	1.0	0	0	0	0	0	100
9[d,e]	K_2CO_3	25	1.0	34	<1	32	0	0	99

[a] CB: carbon balance; [b] No ethanol post-treatment; [c] After reaction, 2 mL ethanol was added into the reaction mixture and stirred (500 rpm) at 25 ºC for 2 h. [d] After reaction, 2 mL ethanol was added into the reaction mixture and stirred at 80 ºC for 2 h. [e] 18-crown-6 (10 mol%) was added together with K_2CO_3 for the reaction.

Table S3. Effect of various hydrosilanes on the conversion of EL to GVL. The reaction conditions are as follows: 1 mmol EL, 1.5 equiv. H^- of hydrosilane, 5 mol% Cs_2CO_3, 2 mL MTHF, 25 ºC, 0.5 h; After reaction, 2 mL ethanol was added into the reaction mixture and stirred at 80 ºC for 2 h.

Hydrosilane name	Structure	EL conv. (%)	GVL yield (%)
Trimethoxysilane	$(MeO)_3SiH$	90	81
Triethoxysilane	$(EtO)_3SiH$	>99	98
Phenylsilane	$PhSiH_3$	99	89
Diphenylsilane	Ph_2SiH_2	45	33
Triethylsilane	Et_3SiH	1	<1
Heptamethyltrisiloxane	Me_3Si-O-MeSiH-O-$SiMe_3$	16	4
Polymethylhydrosiloxane (PMHS)	Me_3Si-O-$(MeSiH\text{-}O)_n$-$SiMe_3$	40	25

Table S4. The synthesis of *N*-substituted lactams from levulinic acid. The reaction conditions are as follows: 1 mmol levulinic acid, 2 mmol amine, 5 mmol HCOOH, 2 mL DMSO, 120 ºC.

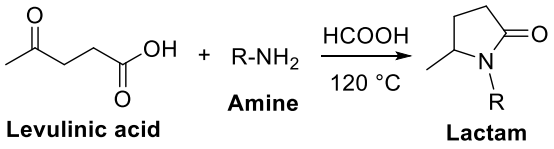

Entry	R	Time (h)	Lactam (%)	
			Yield	Selectivity
1		8	90	95
2		10	87	92
3	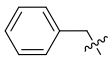	8	92	96
4		10	89	93
5	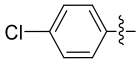	12	85	90

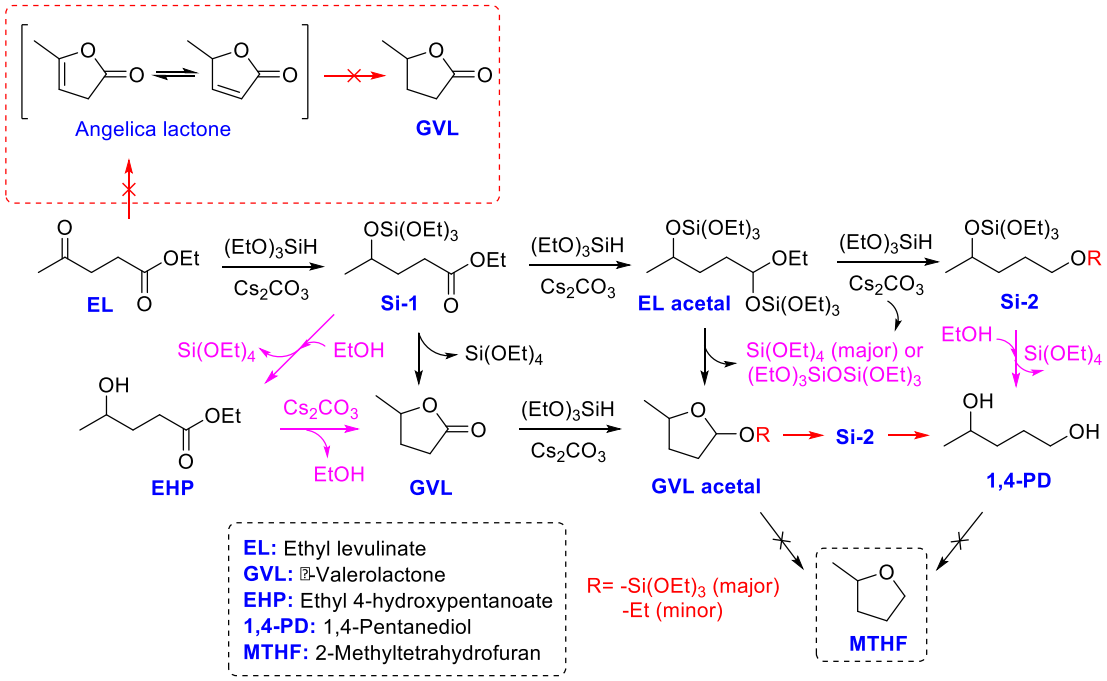

Fig. S1. Reaction pathways for the reduction of EL to GVL and 1,4-PD. The dominant product 1,4-PD with the absence of MTHF formed during the reduction process indicates that the cleavage of the cyclic C-O bond is more apt to take place, as compared with that of the exocyclic C-O bond. GVL acetal and **Si-2** with R = -$Si(OEt)_3$ were the dominant products, which is consistent with the results that $Si(OEt)_4$ instead of $(EtO)_3SiOSi(EtO)_3$ was found to be the major silyl species formed after the reaction.

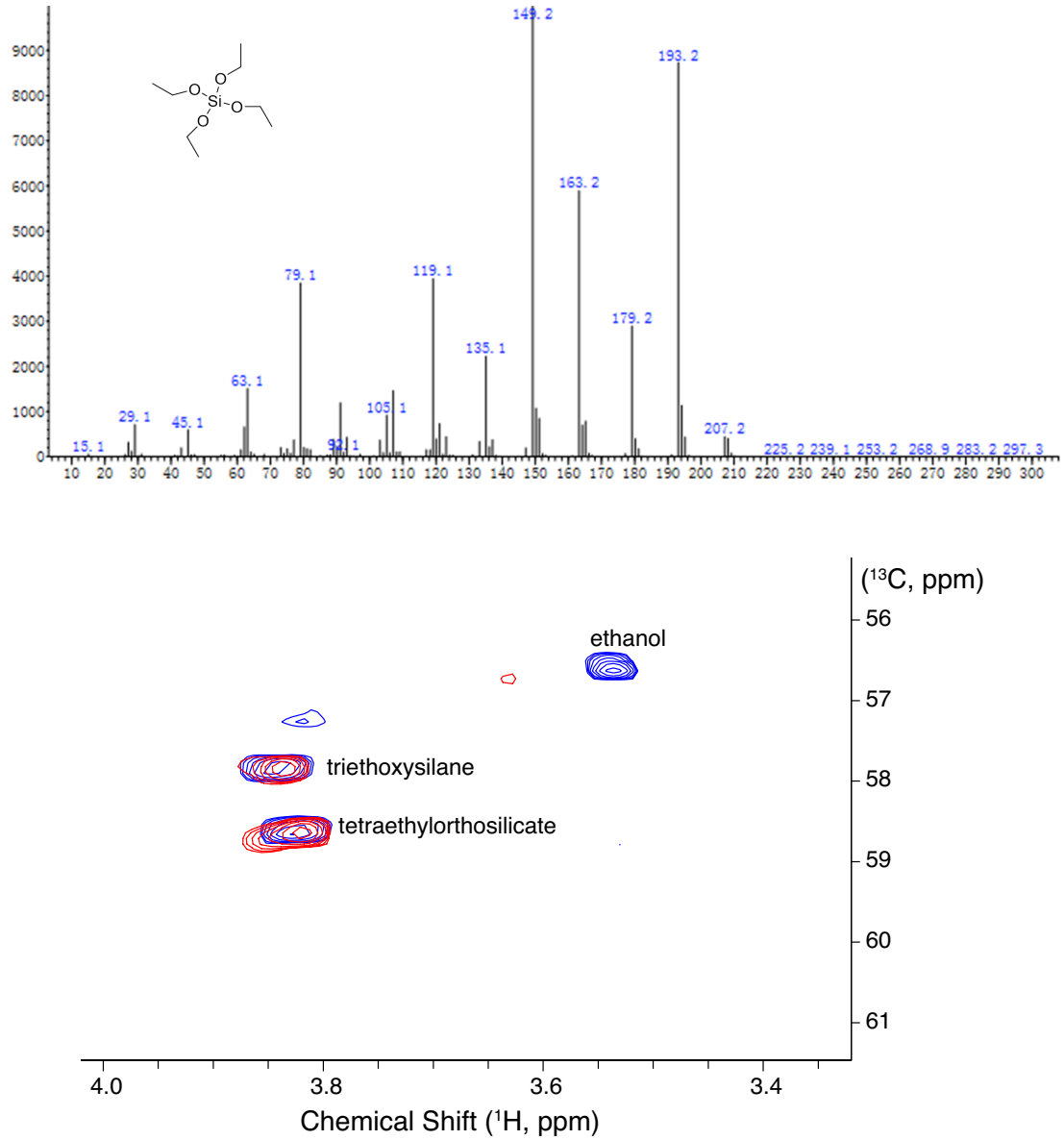

Fig. S2. MS (top) and ^{1}H-^{13}C HSQC NMR (bottom) spectra of tetraethyl orthosilicate Si(OEt)$_4$. For the ^{1}H-^{13}C HSQC NMR spectra, the reaction mixture in red with reference standards in blue is presented, showing tetraethylorthosilicate formation and residual triethoxysilane in the reaction mixture.

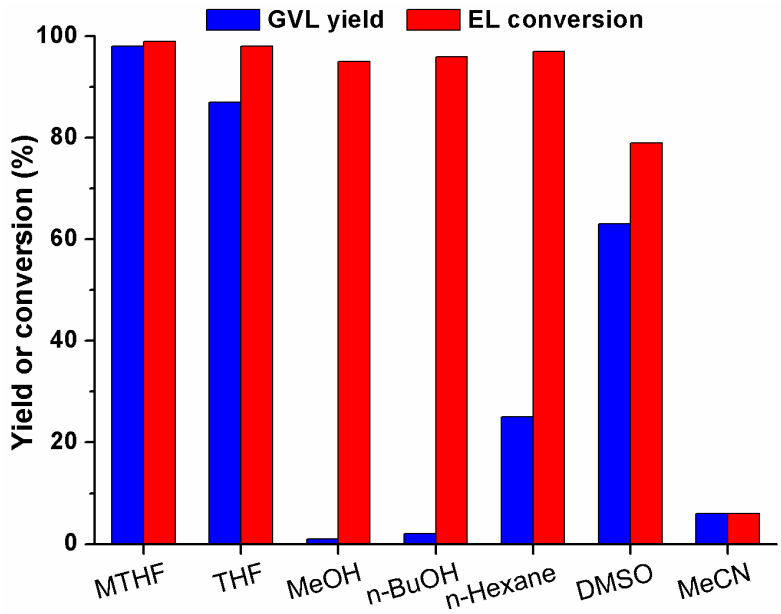

Fig. S3. Effect of various solvents on the hydrogenation of EL to GVL. The reaction conditions are as follows: 1 mmol EL, 1.5 equiv. H^- of $(EtO)_3SiH$, 5 mol% Cs_2CO_3, 2 mL MTHF, 25 ºC, 0.5 h. After the reaction, 2 mL of ethanol was added into the resulting solution and further stirred at 80 ºC for 2 h.

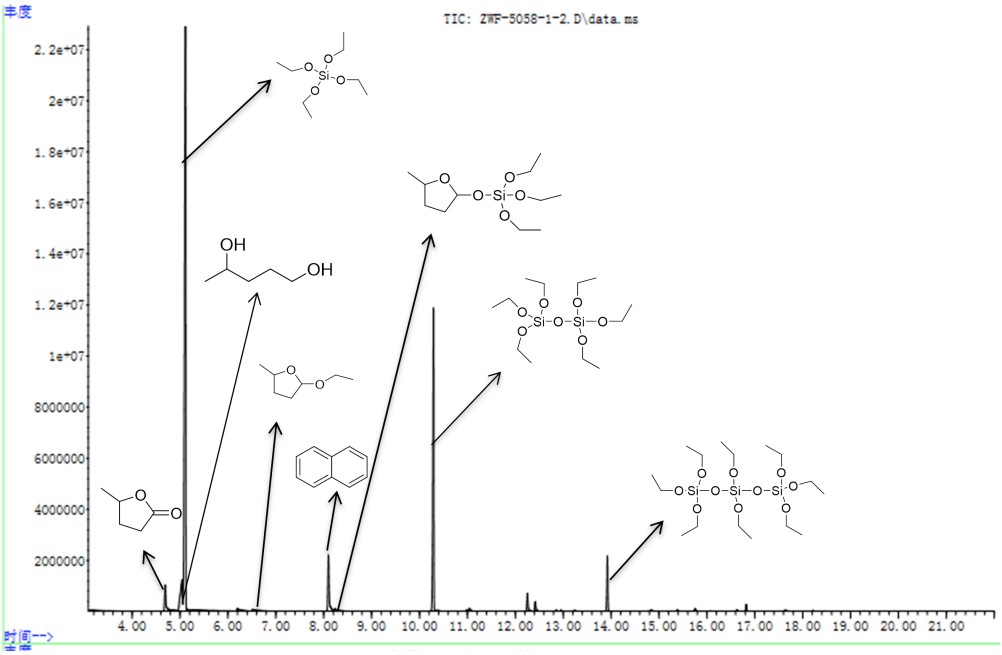

Fig. S4. GC-MS spectrum of the reaction mixture obtained in the hydrogenation of EL in *n*-hexane. Reaction conditions: 1 mmol EL, 1.5 equiv. H^- of $(EtO)_3SiH$, 5 mol% Cs_2CO_3, 2 mL *n*-hexane, 25 ºC, 0.5 h.

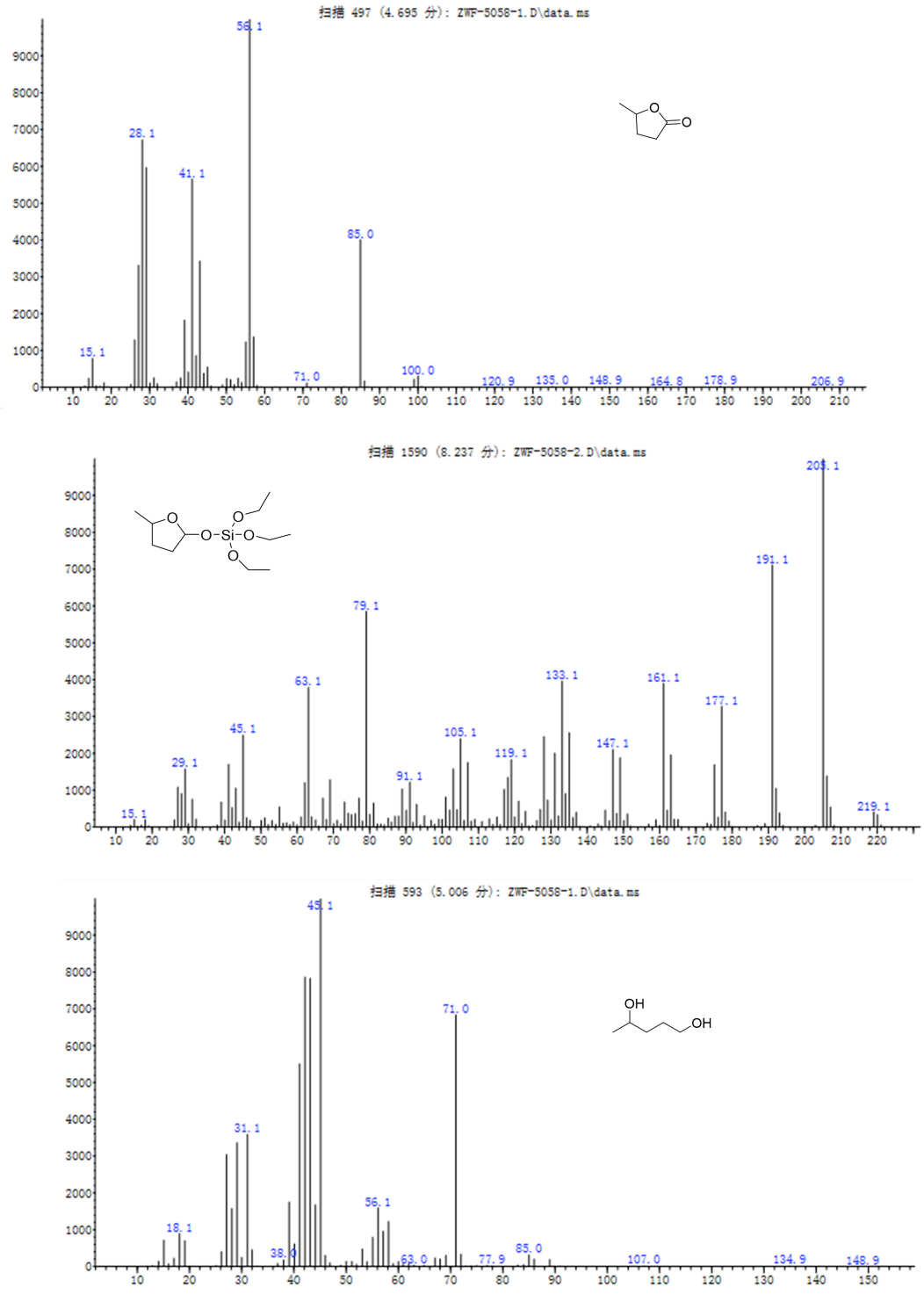

Fig. S5. Selected MS spectra of the products obtained in the hydrogenation of EL in *n*-hexane. Reaction conditions: 1 mmol EL, 1.5 equiv. H^- of $(EtO)_3SiH$, 5 mol% Cs_2CO_3, 2 mL *n*-hexane, 25 ºC, 0.5 h.

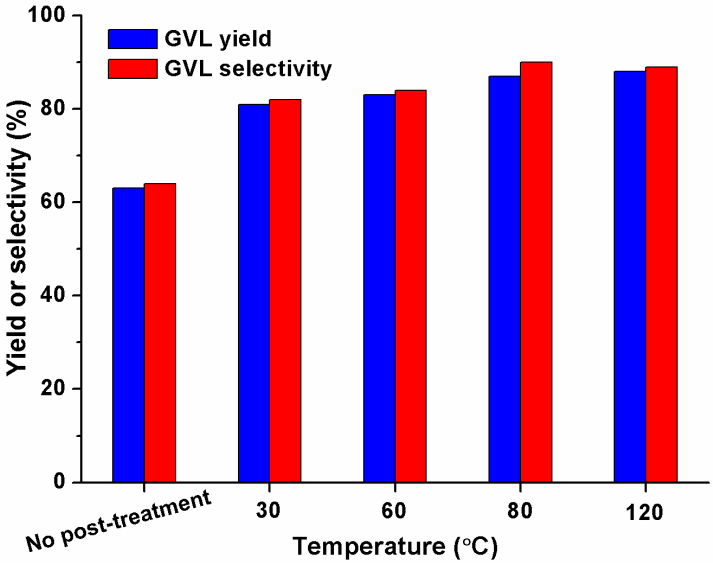

Fig. S6. Effect of post-treatment temperature on the cyclization of *in situ* formed silyl ether (Si-1) to GVL. THF instead of MTHF was used as solvent to check the possibility of MTHF formation with Cs_2CO_3 under otherwise identical conditions listed in Table S2 (GVL acetals were the dominant byproducts, while 1,4-PD and MTHF were not detected by GC-MS in Fig. S7). After the reaction, 2 mL of ethanol was added into the resulting solution and further stirred at the specific post-treatment temperature for 2 h.

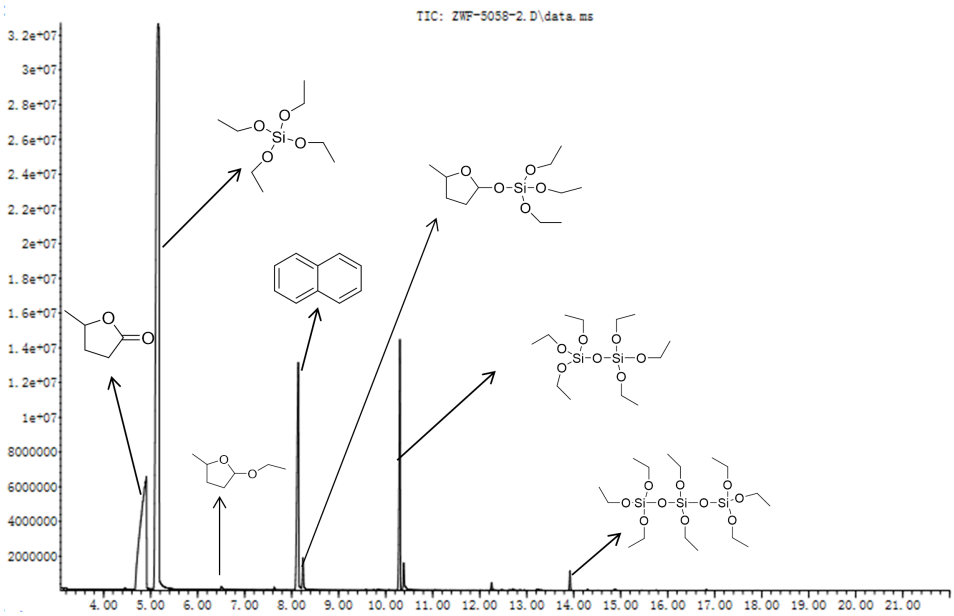

Fig. S7. GC-MS spectrum of the reaction mixture obtained in the hydrogenation of EL in THF. Reaction conditions: 1 mmol EL, 1.5 equiv. H- of $(EtO)_3SiH$, 5 mol% Cs_2CO_3, 2 mL THF, 25 ºC, 0.5 h.

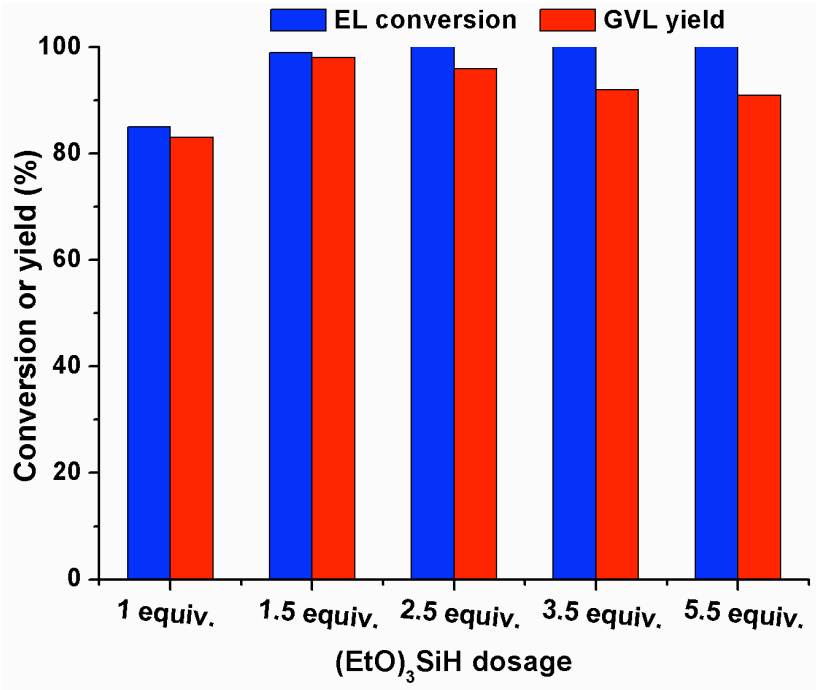

Fig. S8. The effect of hydrosilane dosage on the catalytic hydrogenation of EL. Reaction conditions: 1 mmol EL, 1-5.5 equiv. H^- of $(EtO)_3SiH$, 5 mol% Cs_2CO_3, 2 mL MTHF, 25 ºC, 0.5 h; After reaction, 2 mL ethanol was added into the reaction mixture and stirred at 80 ºC for 2 h.

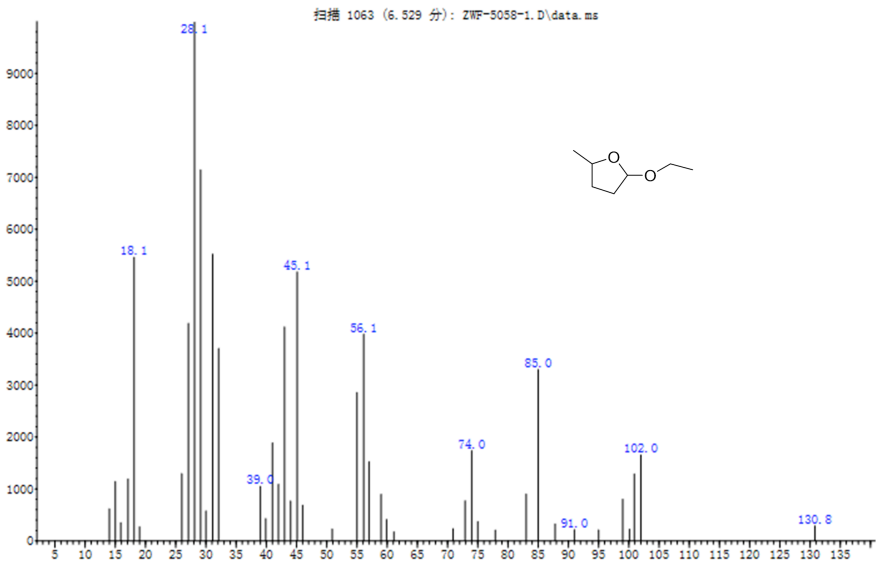

Fig. S9. MS spectrum of GVL ethyl acetal (2-ethoxy-5-methyltetrahydrofuran)

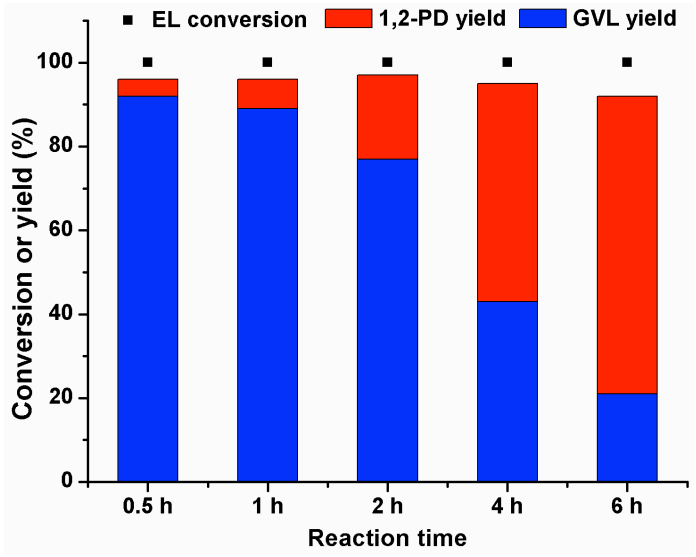

Fig. S10. Effect of reaction time on the hydrogenation of EL. The reaction conditions are as follows: 1 mmol EL, 3.5 equiv. H^- of $(EtO)_3SiH$, 5 mol% Cs_2CO_3, 2 mL MTHF, 25 ºC. After the reaction, 2 mL of ethanol was added into the resulting solution and further stirred at the specific post-treatment temperature for 2 h.

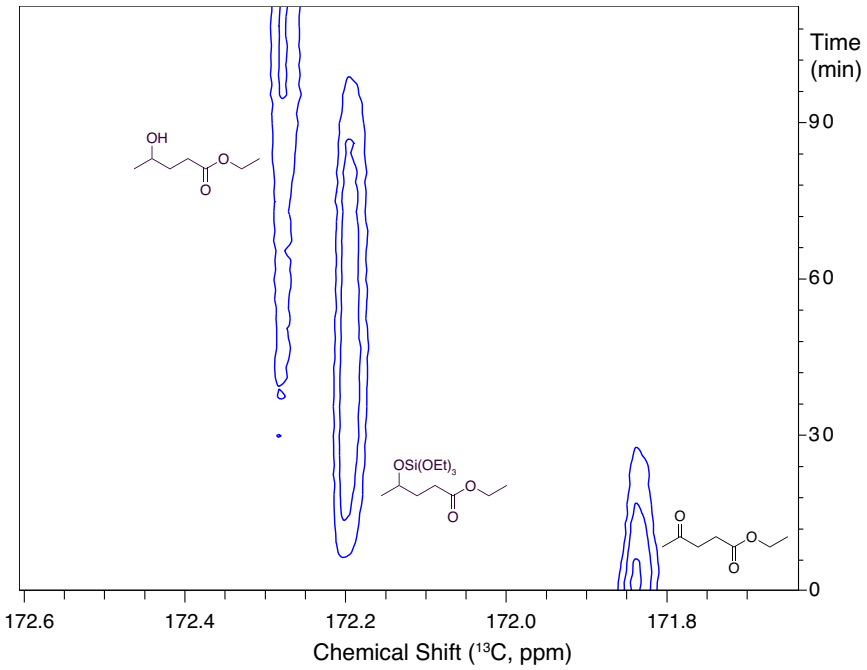

Fig. S11. *In situ* time-series of ^{13}C NMR spectra for the hydrogenation of EL. The used solvent was MTHF with 5% DMSO-d_6, without magnetic stirring.

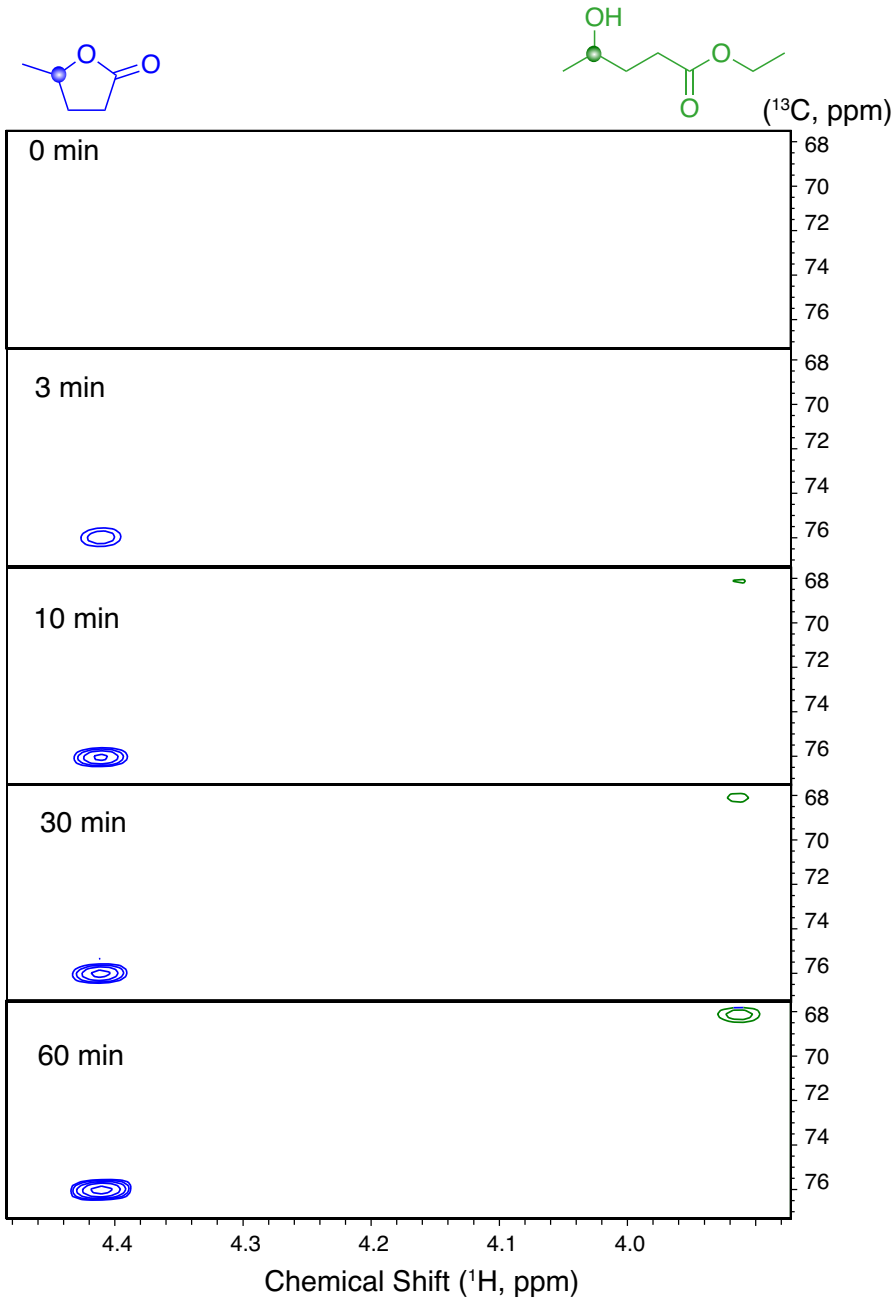

Fig. S12. *Ex situ* NMR spectra of the reaction mixture in the region for the intermediate (ethyl 4-hydroxypentanoate, EHP) and product (γ-valerolactone, GVL). After the indicated reaction times, the reaction mixture was quenched by methanol at room temperature and then sent for NMR analysis. Clearly, better selectivity was observed for the product here than in the NMR tube (Fig. S11).

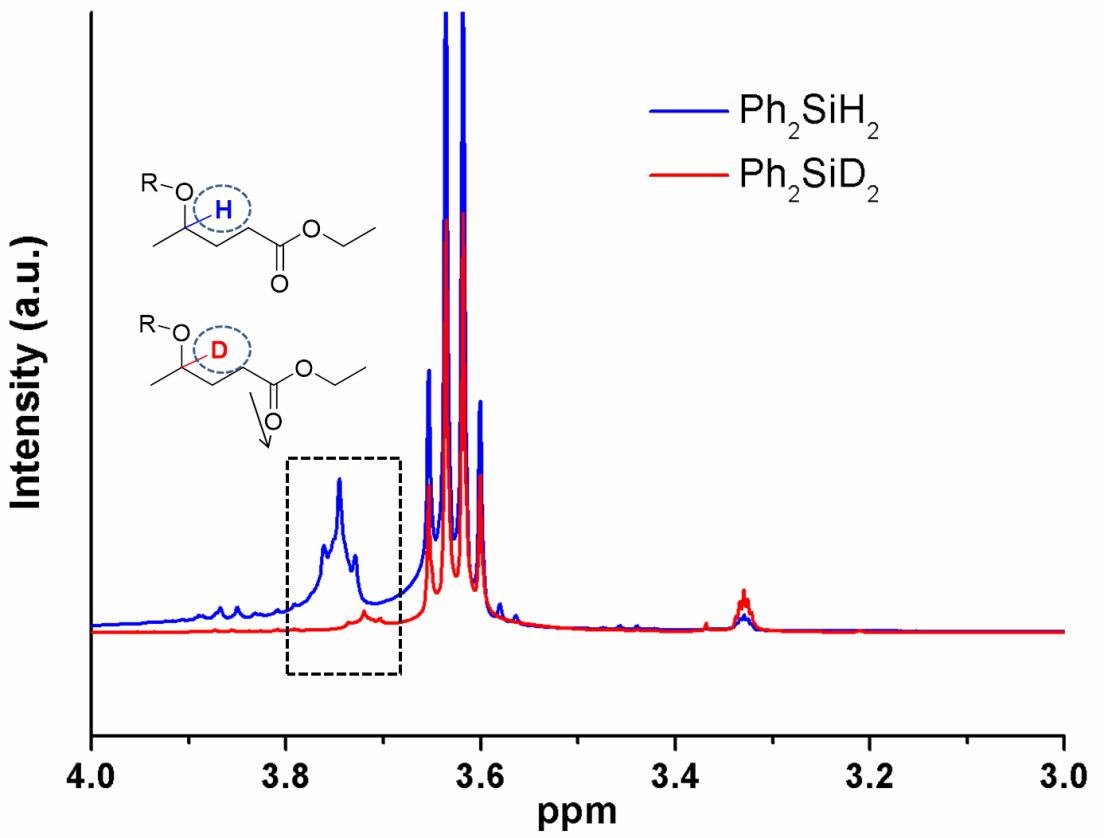

Fig. S13. ^{1}H NMR spectra of the reaction mixture using normal Ph_2SiH_2 and deuterium-labeled Ph_2SiD_2 as reducing agents. THF-d_6 was used as solvent.

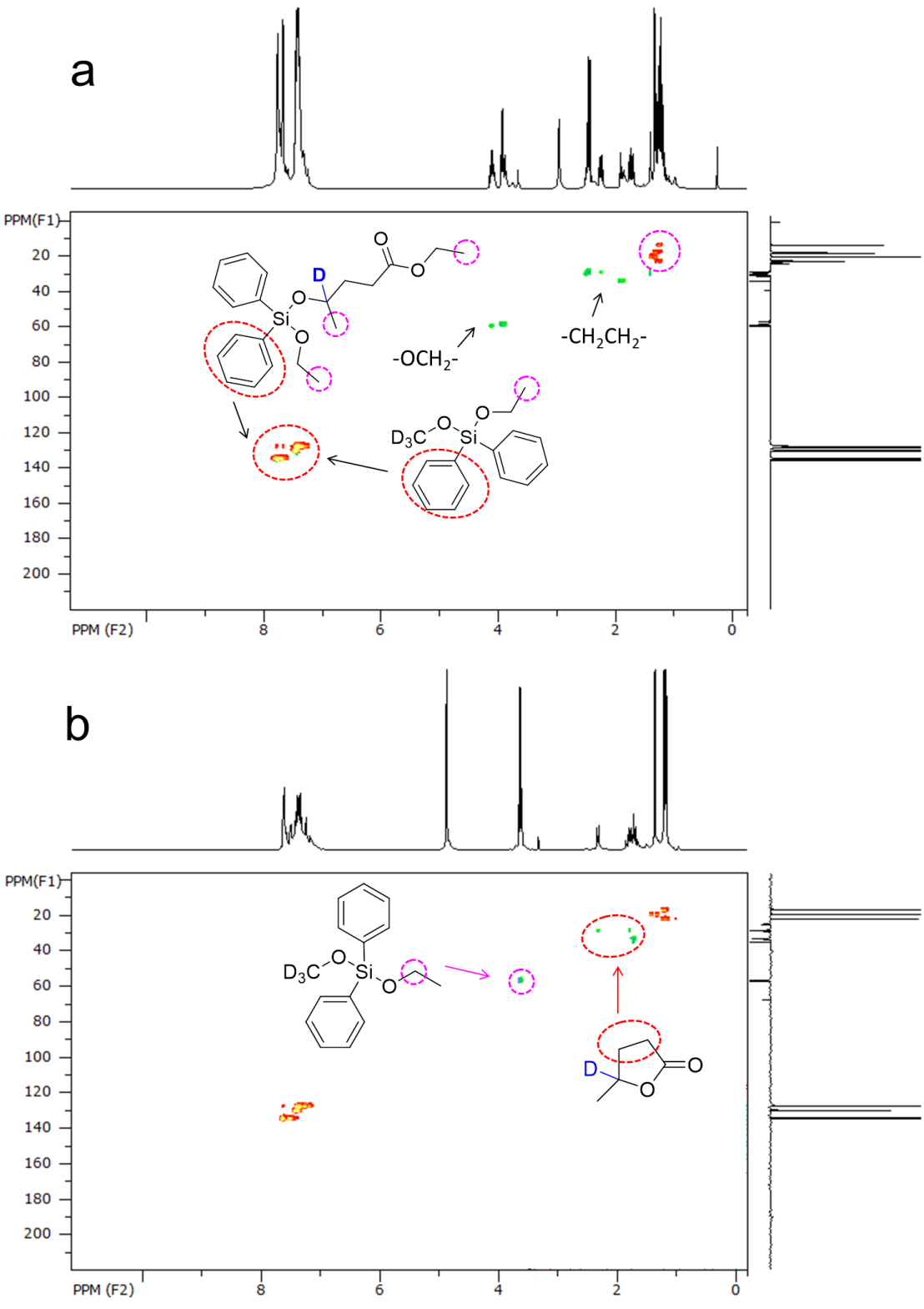

Fig. S14. ^{1}H-^{13}C HSQC NMR spectra of the reaction mixtures using Ph_2SiD_2 as reducing agent. (a) THF-d_6 as solvent and (b) THF-d_6 as solvent with post-treatment by methanol-d_4 at 60 ºC for 2 h.

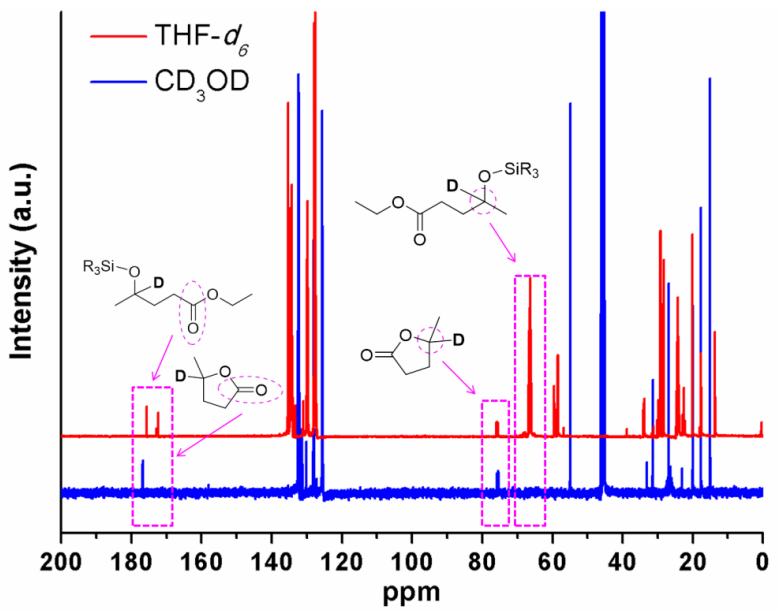

Fig. S15. ^{13}C NMR spectra of the reaction mixtures using Ph_2SiD_2 as reducing agent. THF-d_6 was used as solvent without or with post-treatment by methanol-d_4 at 60 ºC for 2 h.

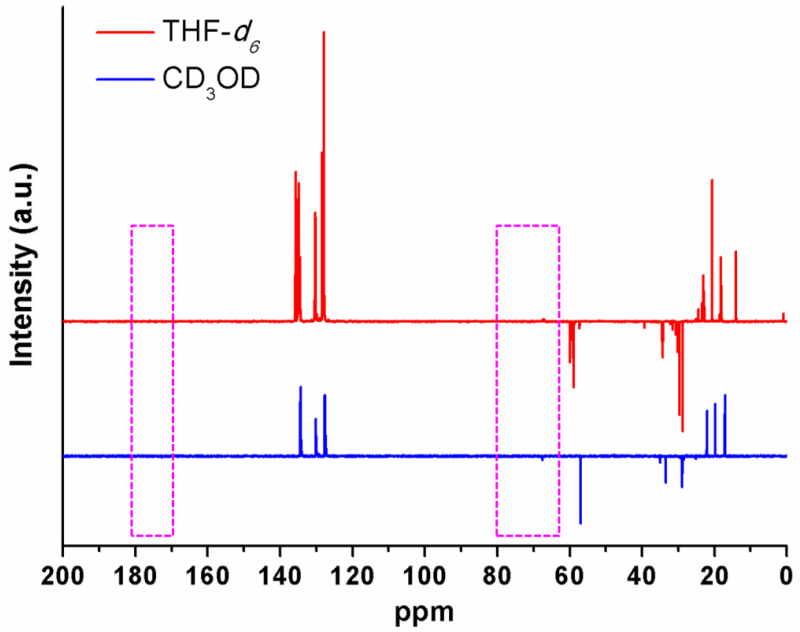

Fig. S16. ^{13}C NMR (DEPT-135) spectra of the reaction mixtures using Ph_2SiD_2 as reducing agent. THF-d_6 was used as solvent without or with post-treatment by methanol-d_4 at 60 ºC for 2 h. Boxes show the absence of quaternary carbon signals present in Fig. S15.

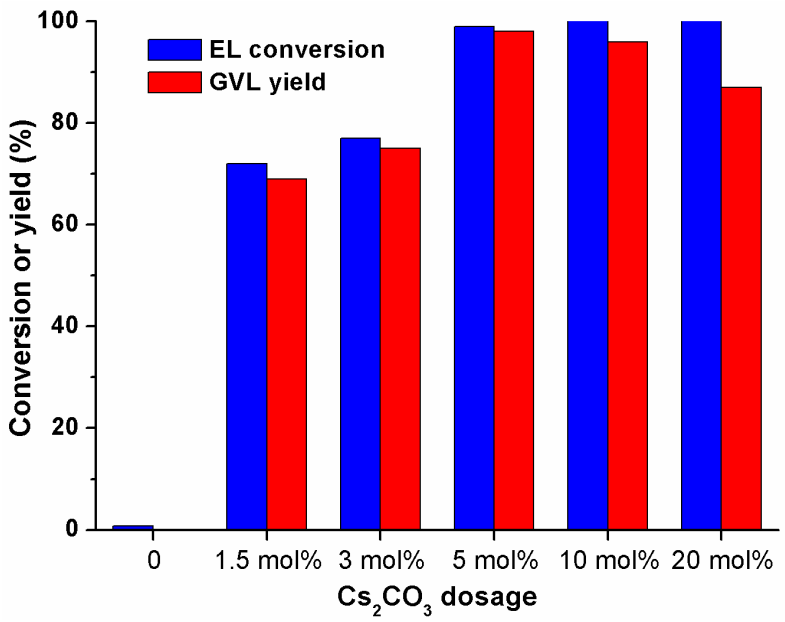

Fig. S17. Effect of Cs_2CO_3 dosage on the conversion of EL to GVL. Reaction conditions: 1 mmol EL, 1.5 equiv. H^-, 2 mL MTHF, 25 ºC, 0.5 h.

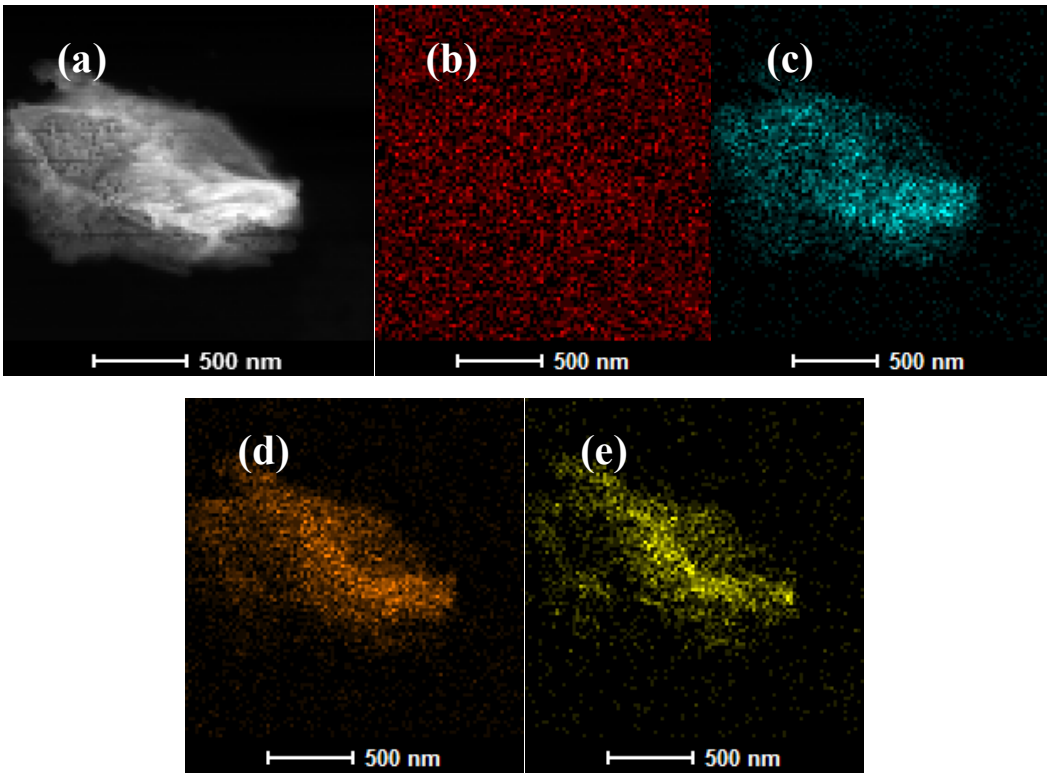

Fig. S18. (a) STEM-HAADF image and (b) C, (c) Cs, (d) O and (e) Si elemental mappings of recovered Cs_2CO_3.

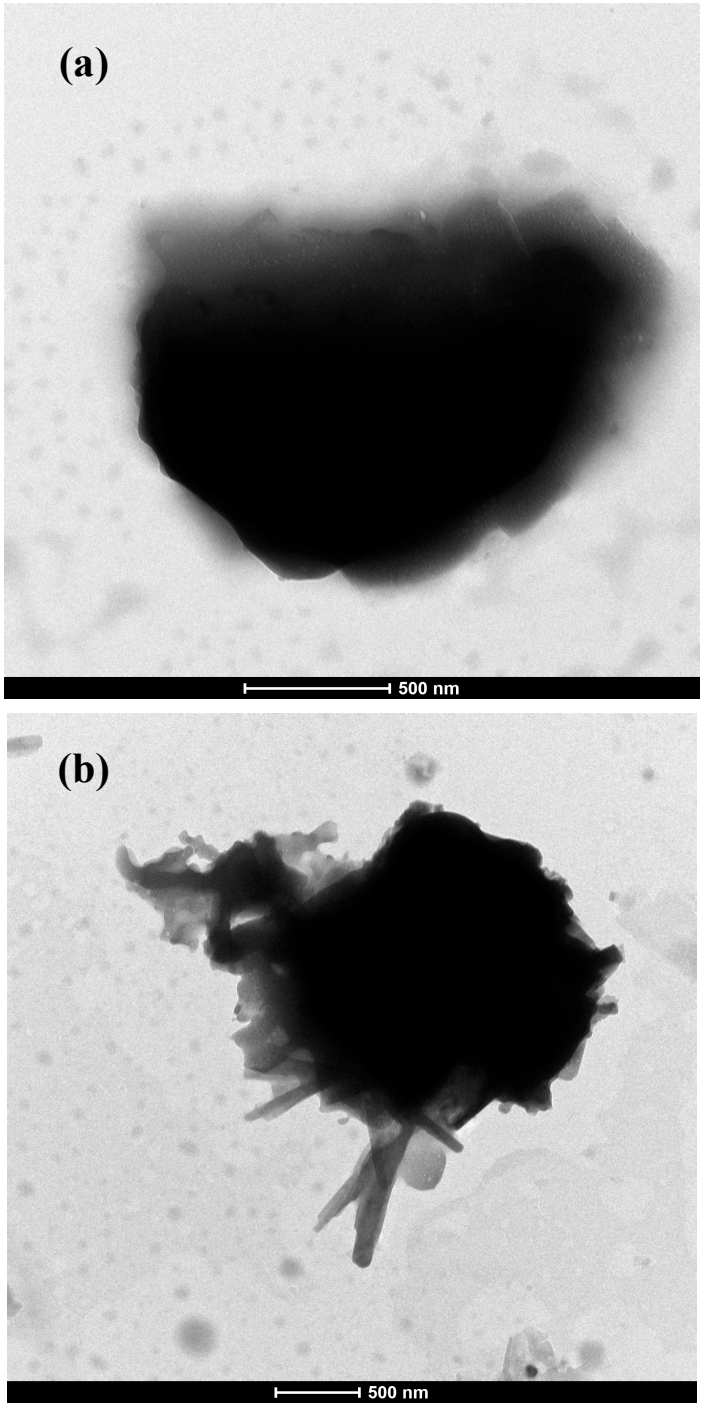

Fig. S19. TEM images of (a) fresh and (b) recovered Cs_2CO_3. Images were taken after dispersion of the solid samples into THF.

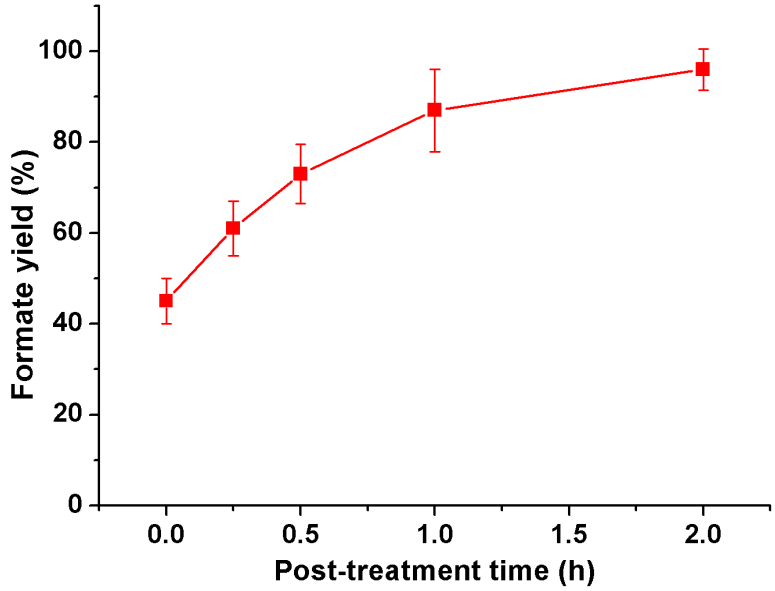

Fig. S20. Effect of post-treatment time on the yield of formate. Reaction conditions: 1 mmol EL, 1.5 equiv. H^- of $(EtO)_3SiH$, 5 mol% Cs_2CO_3, 2 mL MTHF, 25 ºC, 0.5 h. After the reaction, 2 mL ethanol was added into the reaction mixture and stirred at 80 ºC for variable post-treatment time.

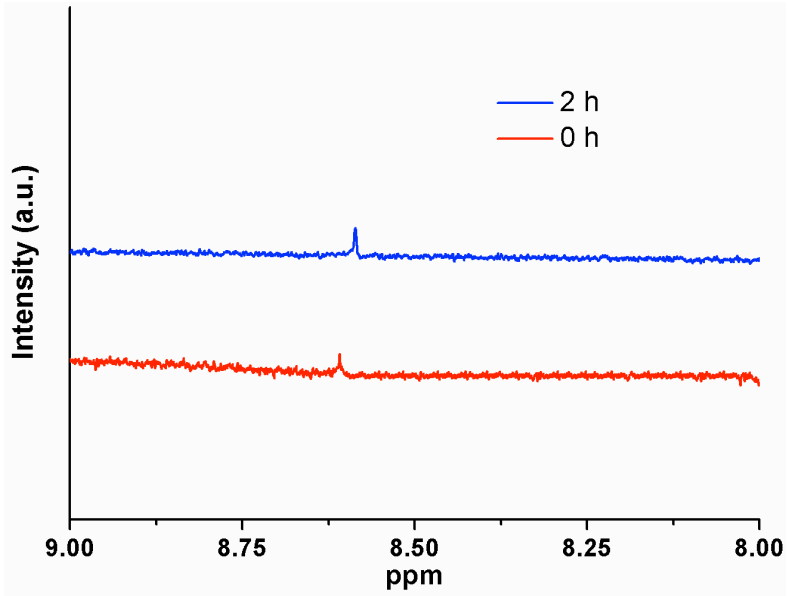

Fig. S21. ^{1}H NMR spectra of the reaction mixture in the chemical shift range of 8-10 ppm for the conversion of EL. Reaction conditions: 1 mmol EL, 1.5 equiv. H^-, 5 mol% Cs_2CO_3, 2 mL MTHF, 25 ºC for 0.5 h. Post-treatment with methanol-d_4 (2 mL) at 80 ºC for 0 or 2 h.

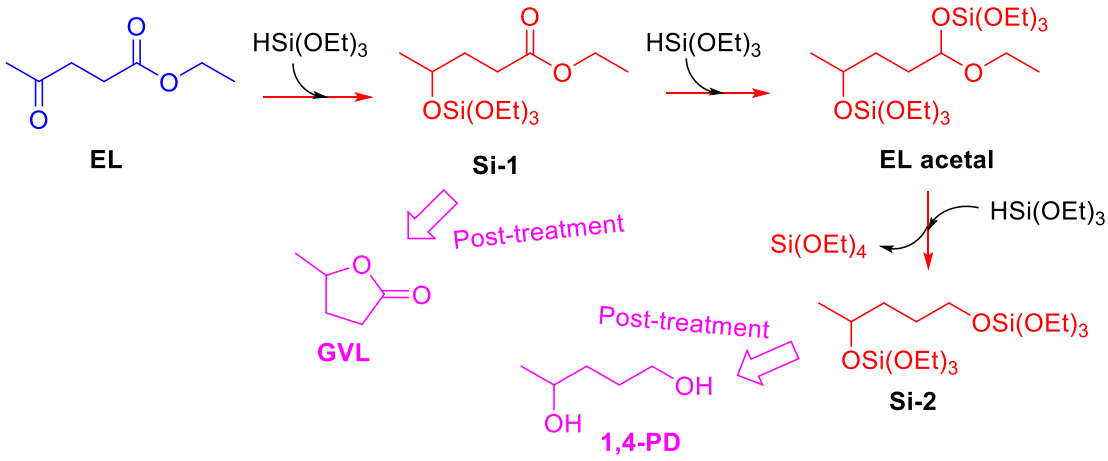

Fig. S22. Reaction pathways for reduction of EL to GVL and 1,4-PD via corresponding silyl ethers.

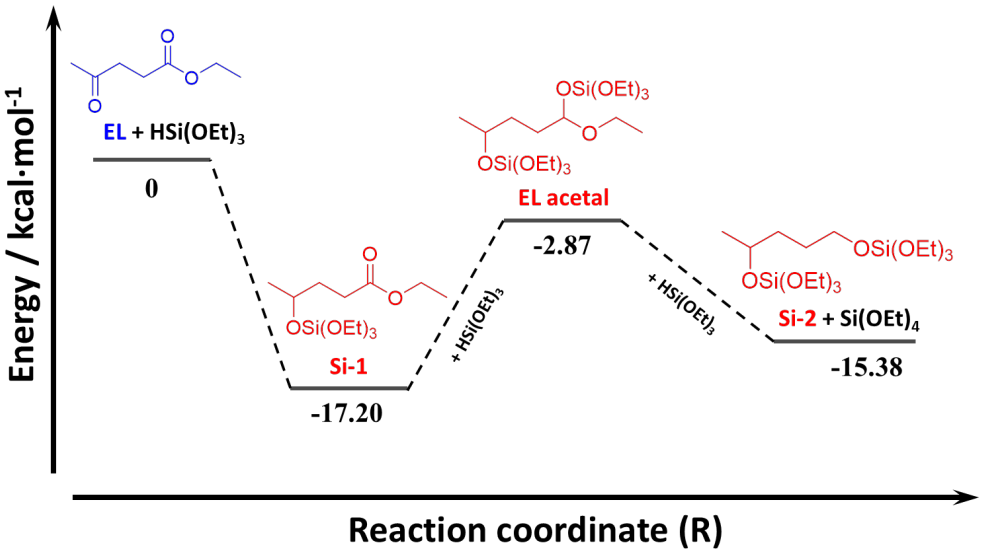

Fig. S23. DFT calculation results of the reaction pathways to different silyl ethers from EL.

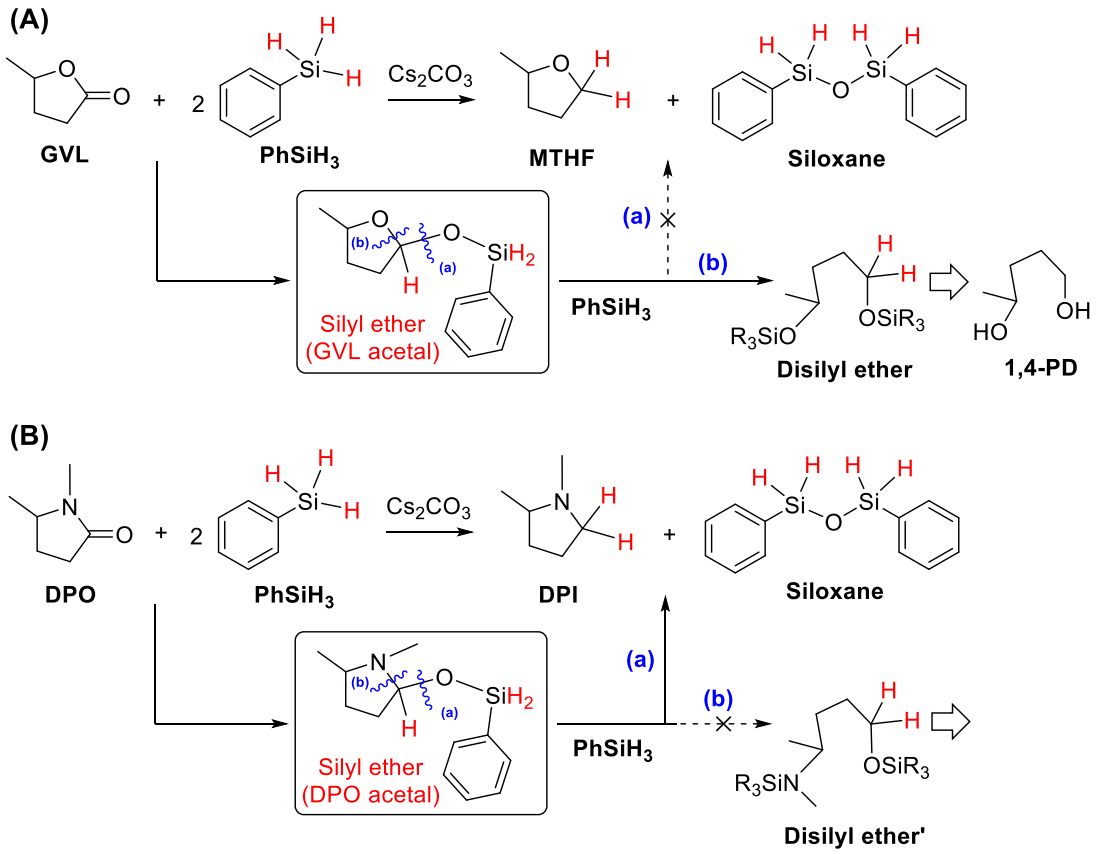

Fig. S24. Reaction pathways for selective reduction of the lactone and lactam via corresponding silyl ethers. (A) Reduction of 1,5-dimethyl-2-pyrrolidinone (DPO) to a) 1,2-dimethylpyrrolidine (DPI) or b) corresponding disilyl ether, and (B) Reduction of valerolactone (GVL) to a) 2-methyltetrahydrofuran (MTHF) or b) corresponding disilyl ether.

References

S1. Gaussian 09, Revision D.01, Frisch, M. J., Trucks, G. W., Schlegel, H. B., Scuseria, G. E., Robb, M. A., Cheeseman, J. R., Scalmani, G., Barone, V., Mennucci, B., Petersson, G. A., Nakatsuji, H., Caricato, M., Li, X., Hratchian, H. P., Izmaylov, A. F., Bloino, J., Zheng, G., Sonnenberg, J. L., Hada, M., Ehara, M., Toyota, K., Fukuda, R., Hasegawa, J., Ishida, M., Nakajima, T., Honda, Y., Kitao, O., Nakai, H., Vreven, T., Montgomery, J. A., Peralta, J. E., Ogliaro, F., Bearpark, M., Heyd, J. J., Brothers, E., Kudin, K. N., Staroverov, V. N., Keith, T., Kobayashi, R., Normand, J., Raghavachari, K., Rendell, A., Burant, J. C., Iyengar, S. S., Tomasi, J., Cossi, M., Rega, N., Millam, J. M., Klene, M., Knox, J. E., Cross, J. B., Bakken, V., Adamo, C., Jaramillo, J., Gomperts, R., Stratmann, R. E., Yazyev, O., Austin, A. J., Cammi, R., Pomelli, C., Ochterski, J. W., Martin, R. L., Morokuma, K., Zakrzewski, V. G., Voth, G. A., Salvador, P., Dannenberg, J. J., Dapprich, S., Daniels, A. D., Farkas, O., Foresman, J. B., Ortiz, J. V., Cioslowski, J., & Fox, D. J. Gaussian, Inc., Wallingford CT, 2013.

S2. X. Chen, L. Zhang, B. Zhang, X. Guo, X. Mu, Highly selective hydrogenation of furfural to furfuryl alcohol over Pt nanoparticles supported on g-C_3N_4 nanosheets catalysts in water. *Sci. Rep.* 2016, **6**, 28558.

S3. J. Wu, G. Gao, J. Li, P. Sun, X. Long, F. Li, *Appl. Catal. B: Environ.* 2017, **203**, 227-236.

S4. M. Hronec, K. Fulajtarová, *Catal. Commun.* 2012, **24**, 100-104.

S5. W. J. Yu, Y. Tang, L. Y. Mo, P. Chen, H. Lou, X. M. Zheng, *Bioresour. Technol.* 2011, **102**, 8241-8246.

S6. M. Hronec, K. Fulajtarová, T. Liptaj, *Appl. Catal. A: Gen.* 2012, **437-438**, 104-111.

S7. L. Deng, Y. Zhao, J. Li, Y. Fu, B. Liao, Q.X. Guo, *ChemSusChem* 2010, **3**, 1172-1175.

S8. X. L. Du, Q. Y. Bi, Y. M. Liu, Y. Cao, K. N. Fan, *ChemSusChem* 2011, **4**, 1838-1843.

S9. A. M. Hengne, C. V. Rode, *Green Chem.* 2012, **14**, 1064-1072.

S10. D. Srimani, A. Mukherjee, A. F. G. Goldberg, G. Leitus, Y. Diskin-Posner, L. J. W. Shimon, Y. B. David, D. Milstein, *Angew. Chem. Int. Ed.* 2015, **54**, 12357-12360.

S11. N. M. Rezayee, D. C. Samblanet, M. S. Sanford, *ACS Catal.* 2016, **6**, 6377-6383.

S12. S. Chakraborty, D. Milstein, *ACS Catal.* 2017, **7**, 3968-3972.

S13. S. Werkmeister, K. Junge, B. Wendt, E. Alberico, H. Jiao, W. Baumann, H. Junge, F. Gallou, M. Beller,. *Angew. Chem. Int. Ed.* 2014, **53**, 8722-8726.